The Journal of Neuroscience, January 1, 2000, 20(1):114–122

Electrophysiological Characterization of Voltage-Gated K^+ Currents in Cerebellar Basket and Purkinje Cells: Kv1 and Kv3 Channel Subfamilies Are Present in Basket Cell Nerve Terminals

Andrew P. Southan and Brian Robertson

Electrophysiology Group, Department of Biochemistry, Imperial College of Science, Technology and Medicine, London SW7 2AY, United Kingdom

To understand the processes underlying fast synaptic transmission in the mammalian CNS, we must have detailed knowledge of the identity, location, and physiology of the ion channels in the neuronal membrane. From labeling studies we can get clues regarding the distribution of ion channels, but electrophysiological methods are required to determine the importance of each ion channel in CNS transmission. Dendrotoxin-sensitive potassium channel subunits are highly concentrated in cerebellar basket cell nerve terminals, and we have previously shown that they are responsible for a significant fraction of the voltage-gated potassium current in this region. Here, we further investigate the characteristics and pharmacology of the voltage-dependent potassium currents in these inhibitory nerve terminals and compare these observations with those obtained from somatic recordings in basket and Purkinje cell soma regions. We find that α-DTX blocks basket cell nerve terminal currents and not somatic currents, and the IC_{50} for α-DTX in basket cell terminals is 3.2 nM. There are at least two distinct types of potassium currents in the nerve terminal, a DTX-sensitive low-threshold component, and a second component that activates at much more positive voltages. Pharmacological experiments also reveal that nerve terminal potassium currents are also markedly reduced by 4-AP and TEA, with both high-sensitivity (micromolar) and low-sensitivity (millimolar) components present. We suggest that basket cell nerve terminals have potassium channels from both the Kv1 and Kv3 subfamilies, whereas somatic currents in basket cell and Purkinje cell bodies are more homogeneous.

Key words: potassium channels; cerebellum; synapse; basket cell; electrophysiology; mouse

A proper understanding of many CNS diseases and disorders requires identification of the ion channels underlying them and knowledge of their normal physiological roles. Recently, considerable progress has been made in understanding certain forms of epilepsy (Biervert et al., 1998; Schroeder et al., 1998; Smart et al., 1998), and episodic ataxia (Browne et al., 1994), both of which may be caused by mutations in genes encoding voltage-gated K (Kv) channels. Kv channels are crucial in regulating neuronal activity. The proteins that comprise these ion channels belong to an extensive and diverse group that exhibits discrete and selective patterns of distribution throughout the brain (e.g., Kv1 subfamily: McNamara et al., 1993, 1996; Wang et al., 1993, 1994; Sheng et al., 1994; Rhodes et al., 1995, 1996; Kv3 subfamily: Weiser et al., 1994; Kv4 subfamily: Sheng et al., 1992). Some Kv channel subtypes are concentrated in specific groups of neurons and are often found tightly clustered within distinct neuronal compartments (Wang et al., 1994; Rhodes et al., 1995). Knowledge of such precise targetting has important implications for defining the roles individual K^+ channels play in regulating neuronal function. Two members of the Kv1 subfamily of potassium channels, Kv1.1 and 1.2, are densely concentrated in the distinctive nerve terminal (*pinceau*) region of cerebellar basket cells, surrounding the axon initial segment of Purkinje neurons (McNamara et al., 1993; Wang et al., 1993). Such a dense concentration would indicate that these channel α-subunits play a significant role in determining membrane excitability in this nerve terminal and in regulating synaptic transmission between basket cells and Purkinje neurons. However, physiological identification of ion channels in CNS nerve terminals is difficult, principally because of their small size, and consequently little direct data are available. Recently we have demonstrated that whole-cell patch-clamp recordings from mouse cerebellar basket cell terminal processes are possible (Southan and Robertson, 1998a), and we showed that α-dendrotoxin (which blocks certain Kv1 subunits) blocks a fraction of voltage-dependent K^+ current in this region. Thus far, presynaptic potassium channels have only been examined using direct patch-clamp recordings from the giant excitatory terminal, the Calyx of Held (Forsythe, 1994); the present study represents the first detailed biophysical and pharmacological characterization of Kv channels in an inhibitory CNS nerve terminal. Direct study of inhibitory, indeed any, CNS nerve terminals is important, because different synaptic terminals have enormously varying properties, dependent on a large number of factors, including target cell, presynaptic anatomy, and precise distribution of their constituent ion channels and receptors (Poncer et al., 1997; Reyes et al., 1998; Walmsley et al., 1998). Our data indicate that in addition to a DTX-sensitive K^+ current, there exists an additional component that has several similarities to cloned channels belonging to the Kv3 subfamily. We also examine the properties of K^+ currents in basket and Purkinje cell somata and contrast these with the basket terminal potassium currents. These data give us an insight into the molecular identities of native K^+

Received July 30, 1999; revised Oct. 15, 1999; accepted Oct. 18, 1999.

We thank the Wellcome Trust for supporting this project (045812) and Bruce Walmsley and Robert Fyffe for helpful discussions.

Correspondence should be addressed to Dr. Brian Robertson, Biochemistry, Imperial College of Science, Technology and Medicine, London SW7 2AY, UK. Email: brian.robertson@ic.ac.uk

Dr. Southan's present address: Channelwork Group, CeNeS Limited, Compass House, Vision Park, Chivers Way, Histon, Cambridge CB4 9ZR, UK.

Copyright © 1999 Society for Neuroscience 0270-6474/99/200114-09$15.00/0

currents in defined regions of an important mammalian CNS circuit.

MATERIALS AND METHODS

Tissue preparation and recording methodology has been previously described in detail (Southan and Robertson, 1998a,b).

Tissue preparation and solutions. Cerebellar slices were prepared from 3- to 5-week-old TO strain male mice (Charles River). After cervical dislocation and decapitation, the brain was immediately dissected out into a chilled (~4°C) oxygenated sucrose-based artificial CSF (ACSF) solution. Parasaggital cerebellar slices (250-μm-thick) were then prepared in cold sucrose ACSF solution (see below) using a Vibroslice (Campden Instruments, Loughborough, UK). A submerged-type incubation chamber containing the standard ACSF solution bubbled with 95% O_2 and 5% CO_2 housed the slices at room temperature (20–23°C) until recordings commenced (20 min to 6 hr maximum after slicing). The standard ACSF contained (in mM): NaCl 124, KCl 3, $NaHCO_3$ 26, NaH_2PO_4 2.5, $MgSO_4$ 2, $CaCl_2$ 2, and D-glucose 10, and was maintained at pH 7.3–7.4 with 95% O_2 and 5% CO_2. The sucrose-based dissection/slicing solution was identical to this standard ACSF with the exception of isosmotic substitution of sodium chloride with sucrose (74.5 gm/l).

Recording apparatus and techniques. For electrophysiological recording, slices were placed in a glass-bottomed recording chamber (volume, ~1 ml) and continuously perfused with ACSF at 3–5 ml/min. Individual neurons and nerve terminals were visualized with differential interference contrast (DIC) optics at 630× overall magnification using an Axioskop FS microscope (Carl Zeiss, Oberkochen, Germany). For somatic recordings, Purkinje cells were readily identified by their large soma (~20 μm diameter) and distinctive distribution in the cerebellar folia; basket cells were identified according to their location in the lower third of the molecular layer and by their characteristic size (soma diameter, ~10 μm). Basket cell nerve terminals could be visualized as fine processes surrounding the Purkinje cell soma, descending to the axon initial segment region (Ramón y Cajal, 1911; Palay and Chan-Palay, 1974). All basket cell soma and nerve terminal recordings were unambiguously confirmed using Lucifer yellow fluorescence microscopy after all electrophysiological measurements had been taken (Southan and Robertson, 1998a).

Recordings were made using patch-clamp techniques with electrodes of resistance between 3 and 6 MΩ for somatic recording and 10–15 MΩ for basket cell nerve terminal recording. All electrodes were fabricated from filamented borosilicate glass (GC150-F10; Clark Electromedical Instruments, Reading, UK) using a PP83 microelectrode puller (Narishige, Tokyo, Japan) and were filled with an intracellular solution consisting of (in mM): KCl 140; $MgCl_2$ 1; $CaCl_2$ 1; EGTA 10; and HEPES 10, pH 7.3. For basket cell recordings, this intracellular solution was supplemented with 1–4 mg/ml Lucifer yellow (Lithium salt; Sigma, Poole, UK) to confirm cell identity after recording.

Electrophysiological recordings were made using an EPC-9 amplifier (Heka Electronik, Lambrecht, Germany), controlled by Pulse software (version 8.05; Heka) running on a Macintosh computer (Power PC, 7500/100). Data were sampled between 4 and 24 kHz after being filtered at one-third the appropriate sampling frequency. Mean series resistance for basket somatic recording was 18 ± 1 MΩ (n = 25), and 75–95% compensation was used. Terminal series resistance (14–30 MΩ) was monitored and compensated for (65–95%) throughout. Where the series resistance of the cells was unstable, recordings were excluded from analysis. Except where indicated, currents were leak-subtracted on-line using a p/4 subtraction routine. Data analysis was performed using Axograph (version 3.5; Axon Instruments, Foster City, CA), Pulsefit (version 8.05; Heka), Igor (version 2.04; Wavemetrics) and Kaleidagraph (version 3.04) software. Data are presented as mean value ± SEM, where n = number of cells. Statistical significance was determined using a Student's t or Wilcoxon signed rank test (Statview II; Abacus Concepts, Calabasas, CA). Activation curves were determined by fitting a Boltzmann expression to calculated conductance (Gv) values. The equation used was: $Gv = G_{max}/\{1 + \exp[-(V - V_{1/2})/k]\}$, where G_{max} is the maximum conductance, V the membrane voltage, $V_{1/2}$ the half activation voltage, and k the slope factor.

Concentration response curves were constructed using the logistic function: Response = maximum response/[1+ (IC_{50}/concentration)], where data were poorly fitted by this equation, a satisfactory fit was obtained from the sum of two separate functions.

Drugs and peptidergic toxins. Toxin I and toxin K were obtained by purification of *Dendroaspis polylepis* venom using previously described methods (Robertson et al., 1996); α-DTX, γ-DTX, charybdotoxin, apamin, agitoxin-2 (AgTX-2), and margatoxin (MgTX) were obtained from Alomone Labs (Jerusalem, Israel). Tetraethylammonium (TEA), 4-aminopyridine (4-AP), and tetrodotoxin (TTX) were obtained from Sigma. All drugs were bath-applied, and salts were ANALAR or equivalent grade and obtained from BDH Chemicals (Poole, UK) or Sigma.

RESULTS

We have recorded from three different membrane locations on two different cell types in the mouse cerebellum, namely Purkinje cell somata, and the somata and terminals of basket cells, which make inhibitory synapses on axosomatic regions of Purkinje cells. To facilitate direct comparisons between K^+ currents, identical solutions and protocols were used throughout. In all basket cell experiments, TTX was included at 1 μM. In Purkinje cell-excised somatic patches, the voltage-gated Na^+ current was negligible (Fig. 1*A*).

Potassium currents in Purkinje somata

Because the whole-cell potassium currents from Purkinje cell somatic recordings are extremely large (peak amplitude often exceeding 15 nA during a step from −90 to +30 mV), we chose to study these currents in outside-out patches, where more satisfactory voltage control could be achieved. Patches were excised within 30 sec of establishing the whole-cell configuration and held at a membrane potential of −90 mV. Virtually all patches pulled off from Purkinje cell somatic regions yielded significant outward currents, most of which had peak amplitudes of >400 pA at +30 mV with patch electrodes of 3–5 MΩ resistance. Mean maximum conductance was 7.5 ± 0.7 nS (n = 6). Potassium conductance–voltage curves were well-fitted with a single, first-order Boltzmann function, yielding a mean $V_{1/2}$ of −17.3 ± 0.7 mV (n = 6) and slope factor (k) of 11.3 ± 0.6 mV (Fig. 1*A; n* = 6). Threshold for current activation was approximately −50 mV. For the voltage step from −90 to −40 mV, mean activation time constant measured by a single exponential fit was 2.9 ± 0.3 msec (n = 6), decreasing exponentially with voltage to 0.2 ± 0.03 msec (n = 6) for the step from −90 to +50 mV (Fig. 2*A*). Single exponentials provided a good fit to the current activation phase (data not shown). Only slight inactivation was seen during 15 msec steps (and then only at more positive voltages); however, more marked current decay was observed on longer (200 msec) voltage steps (Fig. 3*C,E*). Large and rapid tail currents were consistently seen after repolarization to −90 mV.

Somatic and nerve terminal potassium currents in basket cells

Activation curves were constructed for basket cell somatic and nerve terminal voltage-gated potassium currents using whole-cell voltage-clamp data. Currents were obtained from a holding potential of −90 mV, through a series of incrementing voltage steps (+10 mV) up to +50 mV. Conductance was calculated from peak current data for each voltage step and fitted with a Boltzmann equation (see Materials and Methods).

For whole-cell basket somatic currents, maximum conductance was 86.6 ± 17.3 nS (n = 9), and the mean activation curve was fitted with a single Boltzmann function, with a $V_{1/2}$ = −18.4 ± 0.8 mV (n = 9) and slope factor of 13.0 ± 0.7 mV (Fig. 1*B; n* = 9).

In contrast, the conductance–voltage curve obtained from measurements at the nerve terminal was poorly fitted by a single Boltzmann function, and a better fit was obtained with the sum of two Boltzmann functions (Fig. 1*C*). The first component, comprising some 38% of the total curve, had a $V_{1/2}$ = −52.8 ± 2.5 mV (n = 9), with k = 8.3 ± 2.1 mV (n = 9), whereas the second, more

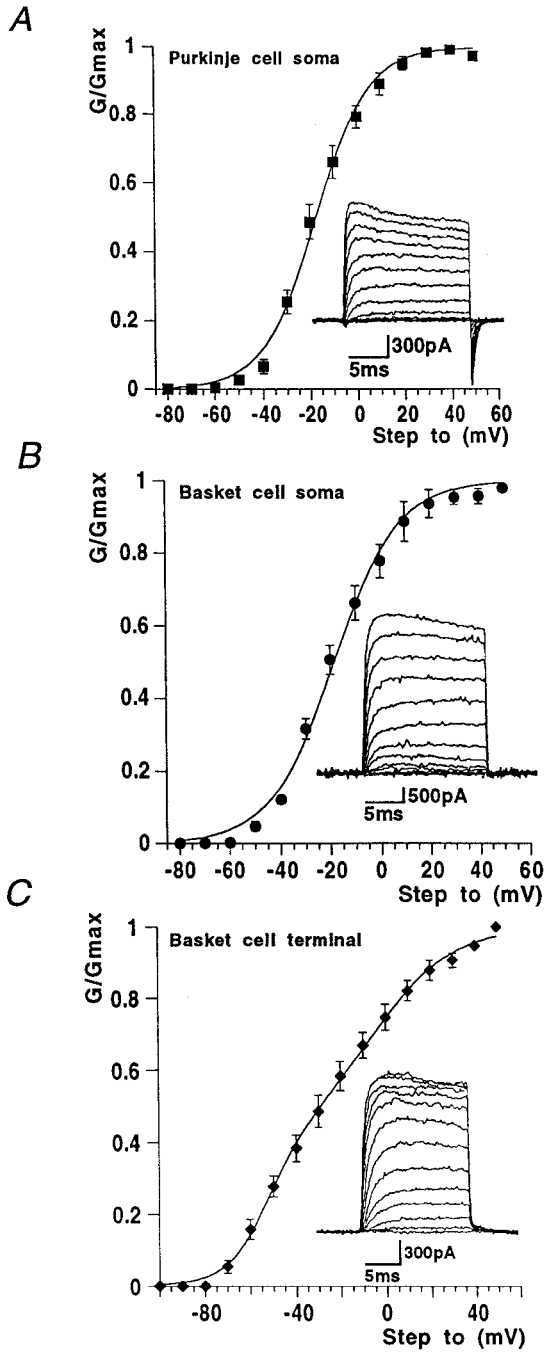

Figure 1. Activation curves from data obtained from soma and nerve terminal recording sites. *Insets* show typical currents recorded from each region using +10 mV incrementing steps to +50 mV from a holding potential of −90 mV. *A*, Purkinje cell soma outside-out voltage-clamp experiments gave activation data with threshold at approximately −50 mV. The Boltzmann function shown superimposed on the data points gave $V_{1/2}$ and slope values quoted in Results. *B*, Whole-cell voltage-clamp responses from the basket cell soma region exhibited similar activation characteristics to Purkinje cell soma responses. *C*, In basket cell terminal recordings, conductance threshold was more negative, approximately −70 mV, and was best fit with the sum of two Boltzmann functions. Values given in Results.

positively activating component (62% of the total K^+ conductance) had a $V_{1/2} = -6.5 \pm 7.3$ mV ($n = 9$), with $k = 18.1 \pm 2.4$ mV ($n = 9$). Maximal conductance for the whole-cell terminal K^+ current was 11.5 ± 1.6 nS. Current threshold was approximately −50 mV for the somatic current and approximately −70 mV for nerve terminal recordings.

For both somatic and terminal recordings, potassium current activation kinetics were rapid, voltage-dependent, and well-fitted by a single exponential function. For the step from −90 to −40 mV, K^+ current activation time constants were 2.6 ± 0.9 ms ($n = 4$), decreasing to 0.5 ± 0.1 msec ($n = 4$) at +50 mV in basket soma (Fig. 2*B*). For K^+ current in basket cell terminal regions, activation time constants were slightly faster, being 1.8 ± 0.3 msec at −40 mV and 0.4 ± 0.02 msec for the step from −90 to +50 mV ($n = 4$; Fig. 2*C*). In mammalian expression systems, Kv1.2 homomeric currents display a remarkable "pulse-potentiation" when activated by strong depolarizing voltage steps at frequencies >1 Hz (Grissmer et al., 1994; P. McIntosh and B. Robertson, unpublished observations. This also occurs in tandem-linked Kv1.1/1.2 channels). Because the basket terminal has a significant proportion of Kv1.2 channel subunits, we were interested to find out whether a similar phenomenon occurred in native membranes. Figure 2*D* shows that when subjected to an identical voltage-stimulation protocol as Kv1.2 channels in cell lines (where an approximately five times enhancement of activation rate was observed), no potentiation occurred; indeed current amplitudes declined slightly with increasing pulse numbers. Similar observations were made in four other nerve terminal recordings.

Basket cell and Purkinje cell somatic current pharmacology

Basket cells

We have previously shown that during 200 msec voltage steps from −90 to +30 mV, the somatic potassium current recorded from basket cells is reduced by high concentrations (10–30 mM) of TEA, yet is insensitive to a number of other potassium channel blockers; namely 4-AP, α-DTX, γ-DTX, Toxin I, Toxin K, apamin, and CbTX (Southan and Robertson, 1998a; see also Table 1 for concentrations). Here, we extend these observations examining margatoxin (MgTX) and agitoxin-2 (AgTX-2), which are reported to be potent blockers of Kv1.1 and Kv1.2 potassium channel subunits in oocytes (Garcia et al., 1994; Hopkins et al., 1996). Additionally, Koch et al., (1997) have shown that considerable MgTX binding is present in the cerebellum. However, at the high concentrations tested here (10 nM), we observed no significant effects of either of these toxins on basket cell somatic potassium current (Table 1).

A full concentration–response relationship for TEA was obtained using outside-out patches ($n = 5$) of somatic membrane obtained from basket cells (Fig. 3*A,B*). Surprisingly, the majority (~80%) of outside-out patches pulled off from basket cell somata yielded no measurable voltage-activated potassium currents, this was in spite of large currents (see above) being present in the whole-cell configuration before the patch was excised. Patches were always pulled off from within the central region of the basket soma. This may suggest that voltage-gated potassium channels in the somatic region of these neurons are clustered in certain "hot" zones on the membrane surface.

In the remaining 20% of excised patches that did exhibit appreciable potassium current during voltage steps from −90 to +30 mV mean control amplitude was 303 ± 177 pA (range, 83–1008 pA; $n = 5$). These currents were blocked by TEA, and the TEA concentration–response curve was fitted with a single

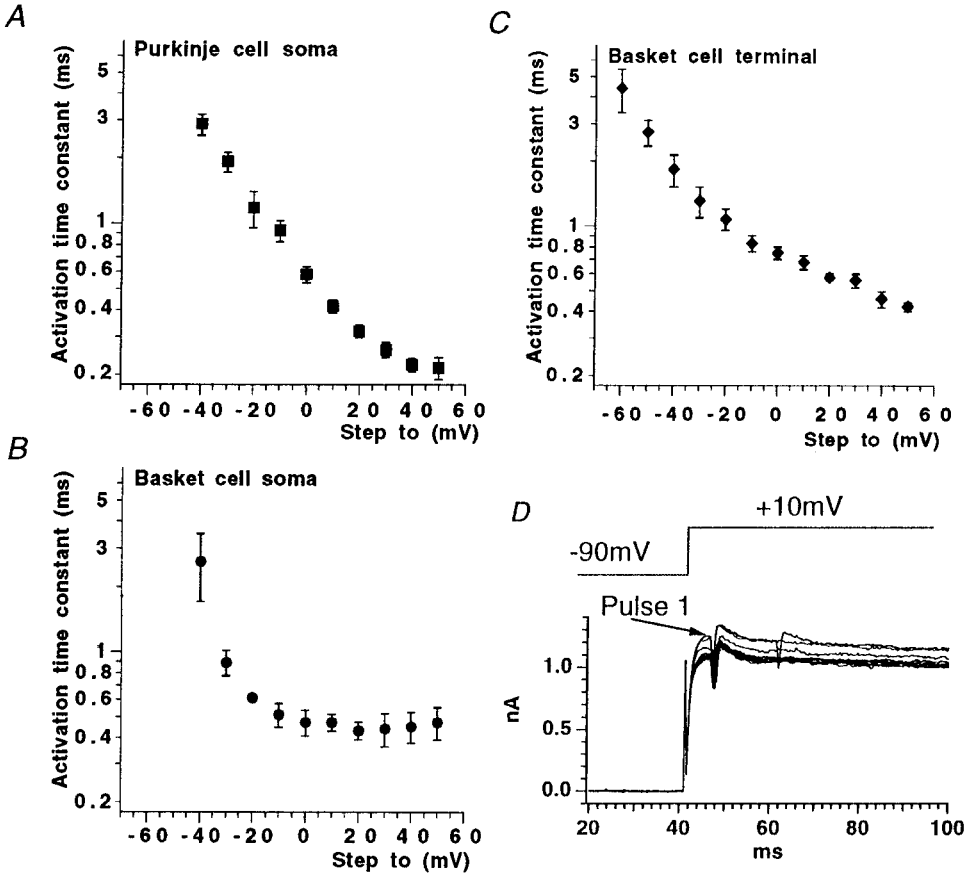

Figure 2. Activation time constant data for Purkinje cell soma and basket cell soma and nerve terminal recording sites. *A*, Purkinje cell soma data. *B*, Basket cell soma data. *C*, Basket cell terminal data. *D,* Repetitive voltage steps to +20 mV from −90 mV evoke total terminal Kv current, which is not potentiated by repetitive pulsing. Note, current traces are not leak-subtracted and also show action currents.

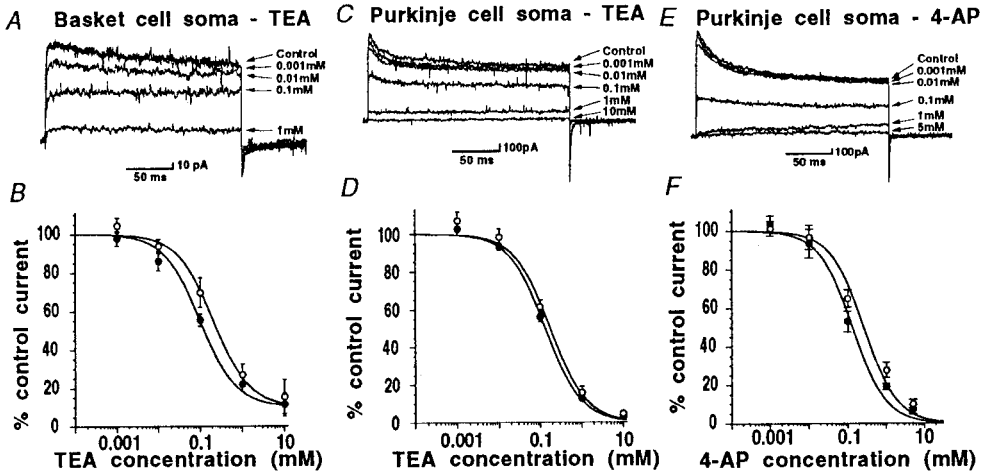

Figure 3. Concentration–response curves for the potassium channel blockers TEA and 4-AP obtained using outside-out patches pulled off from basket cell and Purkinje cell soma regions. *Closed circles* show block of peak current, and *open circles* show block of steady-state current throughout. *A, B*, TEA reduced basket cell somatic currents in a dose-dependent fashion; peak and steady-state current exhibited similar sensitivity. *C, D*, Purkinje cell soma currents were reduced by TEA at concentrations >0.01 mM, again peak and steady-state values were similar, and virtually all of the current was blocked by 10 mM TEA. *E, F*, 4-AP blocks Purkinje cell somatic currents; peak and steady-state current show similar sensitivity to this agent. IC_{50} values quoted in Results were obtained from the fits illustrated here.

component, yielding IC_{50} values of 99 μM for peak current and 206 μM for steady-state current (Fig. 3*A,B; n* = 5). Ninety percent of the total somatic potassium current was blocked by 10 mM TEA. At TEA concentrations >100 μM, the remaining K^+ current was essentially noninactivating. Block by TEA was rapid in both onset and washout (within 10 sec of solution change), and was fully reversible.

Purkinje cells

In these experiments, K^+ current pharmacology was examined using outside-out patches excised from central regions of the Purkinje cell soma, well away from the axon hillock. Voltage-gated K^+ current (200 msec voltage step from −90 to +30 mV) in these isolated membrane patches had a mean amplitude of 668 ± 112 pA (range, 253–1400 pA; *n* = 12). Purkinje soma voltage-activated K^+ current was completely insensitive to α-DTX, Toxin I, Toxin K, and γ-DTX (all at 200 nM). Current was also resistant to block by apamin, CbTX, MgTX, and AgTX-2 (Table 1). However, both TEA and 4-AP were effective blockers of these somatic membrane K^+ currents. For TEA, IC_{50} values were calculated as 131 μM for peak current, similar to the value of 173 μM (*n* = 6) obtained from measurements of block of steady-state current (Fig. 3*C,D*). For the K^+ channel blocker

Table 1. IC_{50} or % of control steady-state current

Blocker	Basket cell soma (whole-cell patch)	Basket cell terminal (whole-cell patch)	Purkinje cell soma (outside-out patch)
TEA	206 μM (outside-out) ($n = 5$)	170 μM/25 mM ($n = 10$)	173 μM ($n = 6$)
4-AP	ne 5 mM ($n = 4$)[a]	8 μM/7.8 mM ($n = 7$)	271 μM ($n = 6$)
α-DTX	ne 200 nM ($n = 5$)[a]	3.2 nM ($n = 6$)	ne 200 nM (101.6 ± 1.6%; $n = 3$)
Toxin K	ne 200 nM ($n = 4$)[a]	56% of control (200 nM; $n = 1$)	ne 200 nM (98.3 ± 3.2; $n = 3$)
γ-DTX	ne 200 nM (94.1 ± 1.7%; $n = 3$)	50% of control (200 nM; $n = 1$)	ne 200 nM (97.6 ± 1.9%; $n = 4$)
Toxin I	ne 200 nM[a] ne 300 nM[a] ($n = 4$)	—	ne 200 nM (92.5 ± 4.1%; $n = 3$)
Apamin	ne 1 μM[a] ($n = 3$)	—	ne 1 μM (93.4 ± 4.5%; $n = 4$)
CbTx	ne 100 nM ($n = 4$)[a]	—	ne 100 nM (98.5 ± 4.0%; $n = 3$)
MgTx	ne 10 nM (96.6 ± 5.3%; $n = 3$)	—	ne 10 nM (94.1 ± 5.6%; $n = 3$)
AgTx-2	ne 10 nM (96.4 ± 2.0%; $n = 3$)	—	ne 10 nM (104.1 ± 4.1%, $n = 3$)

[a]See Southan and Robertson (1998a).

4-AP, IC_{50} values were 133 μM for peak current and 271 μM for steady-state current ($n = 6$; Fig. 3*E,F;* see also Table 1). Once again, block by these agents was rapid in onset and fully reversible, and almost all K current could be blocked at high concentrations of TEA and 4-AP.

Basket cell terminal pharmacology

Recording membrane currents from basket cell terminal processes presents considerable technical obstacles. Their small size (typically ≤2 μm; Ramón y Cajal, 1911; Palay and Chan-Palay, 1974) means visualization, accurate electrode positioning, and successful formation of GΩ seals is particularly challenging, even when using DIC optics and high resistance (up to 15 MΩ), small tip aperture patch electrodes. Confirmation of the identity of the recording site is an absolute requirement when recording from these fine basket cell processes, requiring successful, unambiguous retrograde loading of basket interneurons with an intracellular tracer such as Lucifer yellow during electrophysiological recording. Although the success rate for terminal recordings is extremely low compared to that achievable for somatic recording, we have nevertheless been able to achieve a sufficient number of whole-cell recordings where both high-quality electrophysiological data and certain identification was obtained. We have shown that 200 nM α-DTX rapidly blocks a significant fraction of basket cell terminal potassium current and dramatically increases IPSC frequency and amplitude (Southan and Robertson 1998a,b). Here, we present data for nerve terminal patch-clamp recordings through an extensive range of concentrations of α-DTX (0.1–500 nM; Fig. 4*A,B*). A single component logistic curve fit to these data would indicate that the IC_{50} for α-DTX block of voltage-gated K^+ currents in basket cell terminals is 3.2 nM ($n = 6$). Significantly, the α-DTX-induced block of potassium current is maximal at 50 nM, with no further K^+ current reduction occurring with either 200 or 500 nM. The remaining DTX-insensitive terminal current (40–70%; $n = 7$) was sometimes, although not always, slower to reach peak amplitude, and only very slowly inactivating over the time course of the voltage pulse. Figure 4*C* shows how the terminal potassium steady-state current–voltage relationship is modified after exposure to 200 nM α-DTX ($n = 3$) with the threshold of the remaining potassium current being some 20–30 mV more positive than the threshold of the control current. Fitting Boltzmann curves from these *I–V* data revealed again that control K^+ conductance required two components, with $V_{1/2}$ values of −42 mV ($k = 7$ mV) and −2 mV ($k = 16$ mV) respectively; these values are consistent with those described above under control conditions (see above), whereas the "high-threshold" potassium conductance in 200 nM α-DTX was well-fitted with a single Boltzmann curve, with a $V_{1/2} = +4.1$ mV ($k = 16.2$ mV); $n = 3$ terminals.

Block of "whole terminal" voltage-activated K^+ current by external TEA was tested through a range of concentrations between 0.01 and 30 mM ($n = 3$–7 at each concentration). Block by TEA was also rapid in onset (apparent within 10 sec of solution change), blocking up to a mean of ~70% of the steady-state current at the highest concentration examined. The data points were poorly fitted using a single component logistic curve and are more satisfactorily fit using the sum of two components, with corresponding IC_{50} values for external TEA of 170 μM and 25 mM (Fig. 5*A,B*). The less TEA-sensitive component should be taken as an estimate, because values for inhibition with higher concentrations of TEA were difficult to obtain. Interestingly, 4-AP, which had no effects on basket cell somatic potassium current even at concentrations up to 5 mM (Southan and Robertson 1998a), reduced nerve terminal current at concentrations of ≥10 μM. At the limit of solubility in our ACSF (5 mM), ~60% of the steady-state current was blocked by 4-AP. Block of terminal peak potassium current by 4-AP was not significantly different from

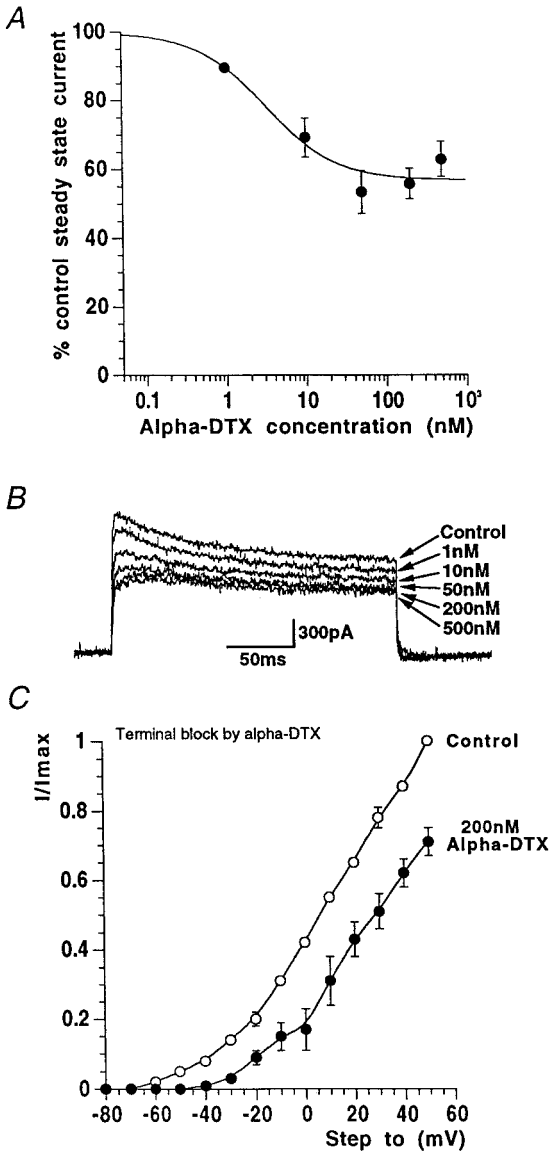

Figure 4. α-DTX blocks a proportion of nerve terminal potassium current. *A*, Concentration–response data showing reduction of nerve terminal potassium steady-state current by α-DTX. The IC_{50} is 3.2 nM. *B*, Example basket cell terminal currents through a range of α-DTX concentrations. *C*, In the presence of a supramaximal concentration of α-DTX, the current–voltage curve is shifted to the right, moving current threshold from approximately −60 to −40 mV for this example ($n = 3$).

that of the steady-state data (200 msec steps). Figure 5, *C* and *D,* shows block of nerve terminal potassium current for a range of concentrations of 4-AP. Mean data points (Fig. 5*C*) were once again poorly fit by a single component curve and were therefore fitted with the sum of two curves. IC_{50} values obtained from this two component logistic fit are 8 μM and 7.8 mM (n = 2–5 terminals).

Figure 6 shows the results of experiments showing that low (1 mM) concentrations of TEA could further block terminal K^+ current already maximally blocked by DTX. In three cells, 200 nM α-DTX was applied to achieve maximal block of the low-threshold Kv current (Fig. 4*B*). Adding 1 mM TEA under such conditions blocked the high-threshold current by ~80% at +50 mV, with no further change in threshold.

To summarize, our pharmacological experiments strongly suggest the presence of two distinct types of voltage-gated K^+ channels in basket cell terminals. These two currents, the DTX-sensitive low-threshold current and the DTX-insensitive, strongly TEA-sensitive high-threshold current, have almost identical $V_{1/2}$ values to those obtained from the activation curve of terminal K^+ conductance (which had two separable components). Additionally, the overall proportions of the currents are in the same range as those obtained from Boltzmann fits. These results give us further confidence that the two components in the Boltzmann fit to terminal K^+ conductance were not an artifact attributable to series resistance problems, or poor space clamp caused by the complicated geometry of the terminals. In the very worst case, uncompensated series resistance would lead to an error of several millivolts with large terminal K^+ currents (~1 nA at very depolarized voltages), which may pull the Boltzmann curve down at positive voltages. However, our results for $V_{1/2}$ values were remarkably consistent both between different cells and also where series resistance and voltage-gated currents were large or small. Furthermore, if our Kv channels were electrotonically dispersed with poor voltage control (as a result of complex terminal morphology), we would not only expect slowing of current activation, but also slowing of current return at the end of the voltage step. This is not seen in our records. Poor space clamp would also lead to greater spread in our values for $V_{1/2}$. Drawing the threads of these different results together leads us to propose that basket cell terminals have at least two separate voltage-gated K^+ channels, in contrast to the somatic regions of basket cells and Purkinje cells, which appear more homogeneous.

DISCUSSION

Here we examine certain properties of Kv currents in three regions of an important cerebellar circuit; Purkinje cell bodies and basket cell bodies and terminals. Our aim is to relate the properties of native Kv currents to channel-mapping studies in the cerebellum and experiments on cloned Kv channels in expression systems, to determine the role of specific potassium channels in cerebellar neuronal integration. It is hoped that such studies will eventually help in understanding how mutations in single Kv genes lead to complex CNS disorders (Cooper and Jan, 1999).

Potassium currents in Purkinje cell bodies

Patch-clamp recordings from these cells revealed a partially inactivating voltage-gated K^+ current that activated with a $V_{1/2}$ = −17 mV, which is similar to results found previously in organotypic slices and cell culture (Gahwiler and Llano, 1989; Hirano and Hagiwara, 1989; Wang et al., 1991; Raman and Bean, 1999). Some of these studies showed a rapidly inactivating Kv current (Gahwiler and Llano 1989; Hirano and Hagiwara, 1989; Wang et al., 1991). Here, inactivation was only significant over longer steps. Our physiological data are similar to those obtained by Raman and Bean (1999), who used whole-cell clamp of dissociated Purkinje cells from slightly younger mice and identified both calcium-dependent and calcium-independent K^+ currents, activating from thresholds of −50 and −40 mV, respectively.

In our pharmacological experiments on Purkinje cell somatic K^+ current, we saw no sensitivity to a variety of DTX homologs, MgTX, AgTX-2, apamin, and CbTX. Only the broad spectrum K^+ channel blockers 4-AP and TEA were effective. There are two likely targets for TEA in Purkinje somatic patches, calcium-activated K^+ current or voltage-gated K^+ current. Under our recording conditions, there is likely to be little or no contribution

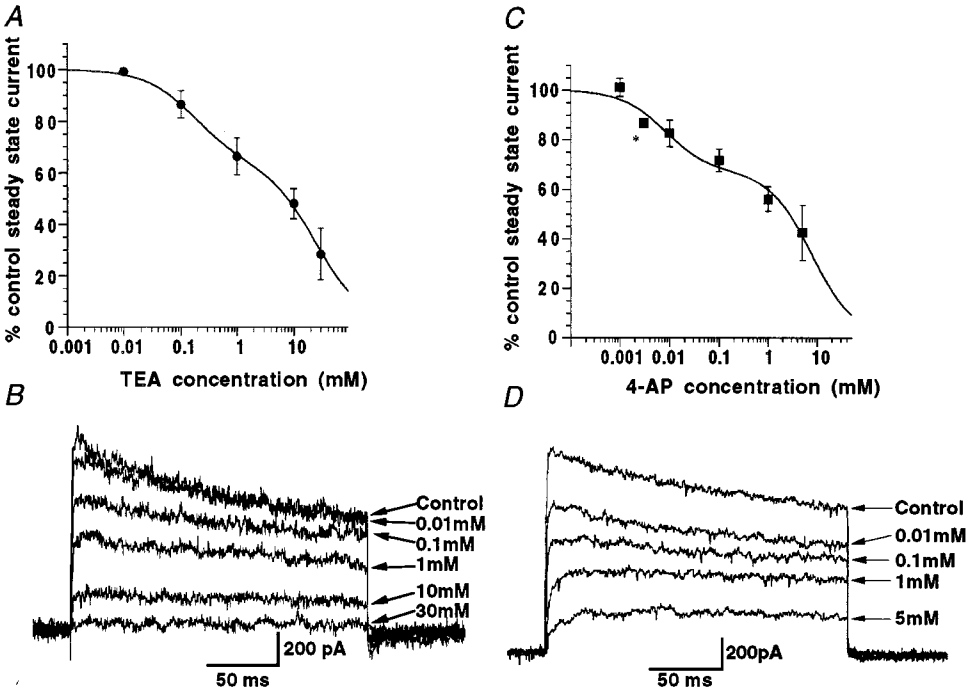

Figure 5. Basket cell nerve terminal currents are blocked by both TEA and 4-AP. *A*, Data from terminals exposed to a range of concentrations of TEA are here fit with the sum of two logistic curves. *B*, Example Kv currents from one terminal exposed to increasing TEA concentrations. *C*, In contrast to the 4-AP insensitivity of the somatic region, basket cell terminal currents exhibit dose-dependent reduction in the presence of 4-AP. Graph shows block of steady-state current data fitted with the sum of two logistic curves. *D*, Example currents from a single nerve terminal experiment through a range of 4-AP concentrations (*denotes $n = 2$ terminals).

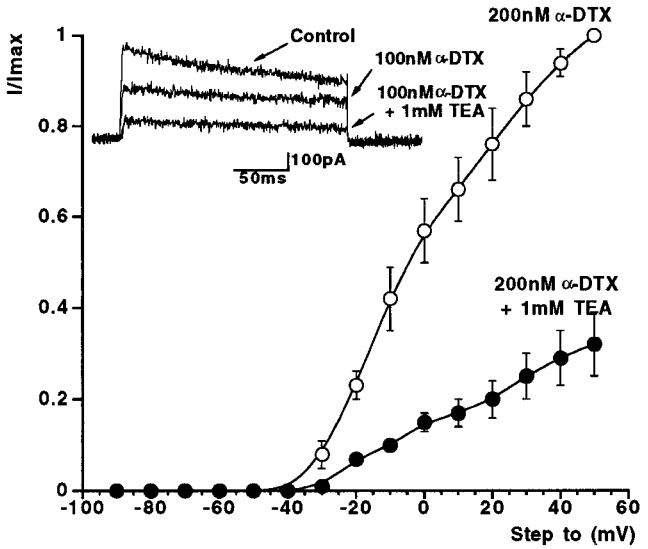

Figure 6. Basket cell terminal current in the presence of α-DTX and after addition of 1 mM TEA. Normalized current–voltage relationship for three cells in a maximal-blocking concentration of α-DTX (200 nM). Note more positive voltage threshold. The remaining DTX-insensitive, high-threshold Kv current is further reduced by 1 mM TEA (see also example traces in *inset*).

from calcium-activated currents. Furthermore, the current was unaffected by either 1 μM apamin or 100 nM charybdotoxin. Our results, showing micromolar sensitivities for TEA and 4-AP, DTX insensitivity, and a fairly positive $V_{1/2}$ value, are consistent with the properties of potassium channels belonging to the Kv3 subfamily. Labeling studies (Goldman-Wohl et al., 1994; Weiser et al., 1994) also indicate that Kv3.3 subunits are present in Purkinje cells.

Potassium current in basket cell somata

Cerebellar basket cells exhibit marked compartmentalization in their voltage-gated K^+ channels. The somatic current is resistant to 4-AP, several dendrotoxin homologs (which are selective for certain Kv1 channels), and certain other peptidergic toxins. Of a wide array of blockers, TEA (IC_{50}, ~200 μM) was the only agent able to inhibit Kv current here. Unfortunately, TEA is not a wholly selective tool, but this high sensitivity invites us to speculate which Kv α-subunits are involved in somatic K^+ current. Some Kv1 channels (Kv1.3, 1.6) generally have sensitivities to TEA in the several millimolar range; only Kv1.1 subunits have submillimolar sensitivity (Chandy and Gutman, 1995; Coetzee et al., 1999), but the absence of DTX sensitivity would exclude Kv1.1 subunits. Kv2 channels require a several millimolar concentration to block, and Kv4 channels also have very little sensitivity to TEA (Coetzee et al., 1999). Perhaps the best candidates come from the Kv3 subfamily, where TEA sensitivities range from 0.1 to 1 mM (Chandy and Gutman 1995; Coetzee et al., 1999). There is little definitive literature with Kv3 antibody labeling in basket cell bodies [although there is some possible somatic labeling with Kv3.2 (Weiser et al., 1994), but none with Kv3.4 (Laube et al., 1996)], but our present electrophysiological evidence showing the midrange $V_{1/2}$ value for somatic current, and especially the absence of 4-AP sensitivity would strongly argue against any known Kv3 α-subunit being involved. This leaves two possibilities, one, that Kv3 channels present in basket cell somata have their properties changed dramatically through coassociation with accessory (β-type) or γ-subunits (Robertson, 1997; Coetzee et al., 1999), or, that another channel subfamily, such as KCNQ2, is present here. KCNQ2 channels are related to the KvLQT family, and in heteromultimers make the "M-current"' (H.-S. Wang et al., 1998). KCNQ2 protein is found in the cerebellum (Biervert et al., 1998; Schroeder et al., 1998; H.-S. Wang et al., 1998), and homomultimers in oocytes have a $V_{1/2}$ of −37 mV (Biervert et al., 1998), with an IC_{50} for TEA of 160 μM (H.-S. Wang et al., 1998), and are insensitive to 2 mM 4-AP (Yang et al., 1998). However, the kinetics of the basket cell somatic Kv current are fast, and KCNQ2 channels in expression systems gate slowly.

Potassium current in terminals

We present here four independent lines of evidence supporting the existence of at least two distinct Kv channel subfamilies present in basket nerve terminals. The activation curve has two components, low-threshold ($V_{1/2}$, approximately −50 mV) and high-threshold ($V_{1/2}$, approximately −4 mV), with the latter being ~60% of the total Kv conductance. Only ~40% of the total outward current could be blocked by α-DTX, with an IC_{50} of 3.2 nM. The α-DTX-insensitive current also activated at more positive voltages ($V_{1/2}$ of −4 mV), and was substantially blocked (~80%) by 1 mM TEA. Concentration–response curves in TEA revealed two components; a high-sensitivity component of ~170 μM and another component in the high millimolar range. The experiments with 4-AP also revealed high- and low-sensitivity components. The simplest explanation for these physiological and pharmacological data is that Kv1 and Kv3 potassium channels constitute most (~85%) of the voltage-gated K^+ current in basket cell terminals. The DTX sensitivity and its IC_{50} value clearly implicates Kv1.1 and 1.2 channel subunits. A heteromultimer containing equal amounts of Kv1.1 and 1.2 α-subunits has TEA sensitivity in the millimolar range and would be less TEA-sensitive with greater numbers of 1.2 subunits in the tetramer (Christie et al., 1990). Such channels would also have 4-AP sensitivity in the millimolar range (Coetzee et al., 1999). There is also overwhelming anatomical evidence for basket cell nerve terminals having substantial amounts of Kv1.2/1.1 protein, often concentrated in "hot spots" (see above). Although our data reveal high levels of certain Kv1 subtypes in basket terminal processes, we are still in the dark as to why these channels are frequently found clustered near specialized junctions (Wang et al., 1994).

There are some unresolved issues however. Kv1.2 channels, expressed in mammalian cell lines, display a remarkable potentiation of current activation rate with voltage pulses delivered at frequencies faster than 1 Hz (Grissmer et al., 1994; McIntosh and Robertson, unpublished observations). No such potentiation of native Kv current was seen in basket cell terminals. Additionally, the DTX-sensitive current has a half activation voltage closer to values for Kv1.1/1.2 channels expressed in *Xenopus* oocytes than the same channels expressed in mammalian cells.

Antibody labeling reveals that Kv3 channel subunits are present in basket cell terminals (Kv3.4: Laube et al., 1996; R. Fyffe, personal communication; Kv3.2b: B. Rudy, personal communication). Kv3.1 and 3.2 proteins are frequently found expressed in axonal/terminal regions in CNS neurons, often GABAergic, that fire at high frequencies (Rudy et al., 1999). Our present data also suggest that Kv3 channels are present, making up ~50% of the total Kv current. The positive $V_{1/2}$ and high TEA and 4-AP sensitivity are all hallmarks of Kv3-type channels (Rudy et al., 1999). Nevertheless, there are some subtle differences between the properties of our terminal current and those results obtained in model systems.

Brew and Forsythe (1995) have identified Kv1 and Kv3 subfamily-like currents in the somata of MNTB neurons in the auditory brainstem, which are important in maintaining fidelity of high-frequency auditory information. It is more difficult to speculate on the possible roles of Kv1 and Kv3 subfamily channels in basket cell terminals. Block of the Kv1 channels with DTX homologs leads to dramatic increases in spontaneous IPSCs in Purkinje cells (Southan and Robertson 1998a,b; Tan and Llano 1999), suggesting a key role for these channels in terminal excitability. Recent two-photon imaging of action potential-evoked calcium rises in basket terminals reveals that DTX did not increase Ca_i; only 4-AP produced dramatic increases in both Ca_i and spontaneous IPSCs (Tan and Llano, 1999). Perhaps then, block of Kv1 subfamily channels alone does not increase calcium entry during action potentials, and possibly these channels are involved in setting resting excitability in terminals and influencing the numbers of "failures" of transmission (Southan and Robertson 1998b; Tan and Llano 1999). Recent work with a Kv1.1-deficient transgenic mouse supports such a model (Zhang et al., 1999).

The role of Kv3 channels in the terminals still eludes us. Although low concentrations of 4-AP increase IPSCs and Ca_i levels (Tan and Llano, 1999), low concentrations of TEA have only modest effects on spontaneous IPSCs (Southan and Robertson, 1998b; Tan and Llano, 1999). It is possible that Kv3 channel block may only have effects on high-frequency trains in basket cells (L.-Y. Wang et al., 1998). Direct studies with paired recordings and ideally selective blockers of Kv3 channels, will be required to fully address this. Our present data, being the first electrophysiological and pharmacological characterization of Kv currents in inhibitory nerve terminals, will hopefully increase our understanding of the roles played by such currents in fast synaptic transmission at CNS synapses.

REFERENCES

Biervert C, Schroeder BC, Kubisch C, Berkovic SF, Propping P, Jentsch TJ, Steinlein OK (1998) A potassium channel mutation in neonatal human epilepsy. Science 279:403–406.

Brew HM, Forsythe ID (1995) Two voltage-dependent K^+ conductances with complementary functions in postsynaptic integration at a central auditory synapse. J Neurosci 15:8011–8022.

Browne DL, Gancher ST, Nutt JG, Brunt ER, Smith EA, Kramer P, Litt M (1994) Episodic ataxia/myokymia syndrome is associated with point mutations in the human potassium channel gene KCNA1. Nat Genet 8:136–140.

Chandy KG, Gutman GA (1995) Voltage-gated potassium channel genes. In: Handbook of receptors and channels (North RA, ed) pp 1–71. Boca Raton, FL: CRC.

Christie MJ, North RA, Osborne PB, Douglass J, Adelman JP (1990) Heteropolymeric potassium channels in Xenopus oocytes from cloned subunits. Neuron 2:405–411.

Coetzee WA, Amarillo Y, Chiu J, Chow A, Lau D, McCormack T, Moreno H, Nadal MS, Ozaita A, Pountney D, Saganich M, Vega-Saenz de Miera E, Rudy B (1999) Molecular diversity of K^+ channels. Ann NY Acad Sci 868:233–285.

Cooper EC, Jan LY (1999) Ion channel genes and human neurological disease: recent progress, prospects, and challenges. Proc Natl Acad Sci USA 96:4759–4766.

Forsythe ID (1994) Direct patch recording from identified presynaptic terminals mediating glutamatergic EPSCs in the rat CNS, *in vitro*. J Physiol (Lond) 479:381–387.

Gahwiler BH, Llano I (1989) Sodium and potassium conductances in somatic membranes of rat Purkinje cells from organotypic cerebellar cultures. J Physiol (Lond) 417:105–122.

Garcia ML, Garcia-Calvo M, Hidalgo P, Lee A, MacKinnon R (1994) Purification and characterization of three inhibitors of voltage-dependent K^+ channels from *Leiurus quinquestriatus* var. hebraeus venom. Biochemistry 33:6834–6839.

Goldman-Wohl DS, Chan E, Baird D, Heintz N (1994) Kv3.3b: a novel *Shaw* type potassium channel expressed in terminally differentiated cerebellar Purkinje cells and deep cerebellar nuclei. J Neurosci 14:511–522.

Grissmer S, Nguyen AN, Aiyar J, Hanson DC, Mather RJ, Gutman GA, Karmilowicz MJ, Auperin DD, Chandy KG (1994) Pharmacological characterization of five cloned K^+ channels, types Kv1.1, 1.2, 1.3, 1.5 and 3.1, stably expressed in mammalian cell lines. Mol Pharmacol 45:1227–1234.

Hirano T, Hagiwara S (1989) Kinetics and distribution of voltage-gated Ca, Na and K channels on the somata of rat cerebellar Purkinje cells. Pflügers Arch 413:463–469.

Hopkins W, Miller JL, Miljanich GP (1996) Voltage-gated potassium channel inhibitors. Curr Pharm Des 2:389–396.

Koch R, Wanner SG, Koschak A, Hanner M, Schwarzer C, Kaczorowski GJ, Slaughter RS, Garcia ML, Knaus HG (1997) Complex subunit assembly of neuronal voltage-gated K^+ channels. J Biol Chem 272:27577–27581.

Laube G, Röper J, Pitt JC, Sewing S, Kistner U, Garner CC, Pongs O, Veh RW (1996) Ultrastructural localization of *Shaker*-related potassium channel subunits and synapse-associated protein 90 to septate-like junctions in rat cerebellar Pinceaux. Mol Brain Res 42:51–61.

McNamara NMC, Muniz ZM, Wilkin GP, Dolly JO (1993) Prominent location of a K^+ channel containing the α-subunit Kv1.2 in the basket cell nerve terminals of rat cerebellum. Neuroscience 57:1039–1045.

McNamara NMC, Averill S, Wilkin GP, Dolly JO, Priestley JV (1996) Ultrastructural localization of a voltage-gated K^+ channel α subunit (Kv1.2) in the rat cerebellum. Eur J Neurosci 8:688–699.

Palay SL, Chan-Palay V (1974) Cerebellar cortex. Cytology and organization. Berlin: Springer.

Poncer JC, McKinney RA, Gahwiler BH, Thompson SM (1997) Either N- or P-type calcium channels mediate GABA release at distinct inhibitory synapses. Neuron 18:463–472.

Raman IM, Bean BP (1999) Ionic currents underlying spontaneous action potentials in isolated cerebellar Purkinje neurons. J Neurosci 19:1663–1674.

Ramón y Cajal S (1911) Histology of the nervous system of man and vertebrates, (Swanson N, Swanson L, translators). Oxford: Oxford UP.

Reyes A, Lujan R, Rozov A, Burnashev N, Somogyi P, Sakmann B (1998) Target-cell-specific facilitation and depression in neocortical circuits. Nat Neurosci 1:279–285.

Rhodes KJ, Keilbaugh SA, Barrezueta NX, Lopez KL, Trimmer, JS (1995) Association and colocalisation of K^+ channel α- and β-subunit polypeptides in rat brain. J Neurosci 15:5360–5371.

Rhodes KJ, Monaghan MM, Barrezueta NX, Nawoschick S, Bekele-Arcuri Z, Matos MF, Nakahira K, Schechter LE, Trimmer JS (1996) Voltage-gated K^+ channel β subunits: expression and distribution of Kvβ1 and Kvβ2 in adult rat brain. J Neurosci 16:4846–4860.

Robertson B (1997) The real life of voltage-gated potassium channels: more than model behaviour. Trends Pharmacol Sci 18:474–483.

Robertson B, Owen D, Stow J, Butler C, Newland C (1996) Novel effects of dendrotoxin homologues on subtypes of mammalian Kv1 potassium channels expressed in *Xenopus* oocytes. FEBS Lett 383:26–30.

Rudy B, Chow A, Lau D, Amarillo Y, Ozaita A, Saganachi M, Moreno H, Nadal MS, Hernandez-Pineda R, Hernandez-Cruz A, Erisir A, Leonard C, Vega-Saenz de Miera E (1999) Contributions of Kv3 channels to neuronal excitability Ann NY Acad Sci 868:304–343.

Schroeder BC, Kubisch C, Stein V, Jentsch TJ (1998) Moderate loss of function of cyclic-AMP-modulated KCNQ2/KCNQ3 K^+ channels causes epilepsy. Nature 396:687–690.

Sheng M, Tsaur M-L, Jan YN, Jan, LY (1992) Subcellular segregation of two A-type K^+ channel proteins in rat central neurons Neuron 9:271–284.

Sheng M, Tsaur M-L, Jan YN, Jan, LY (1994) Contrasting subcellular localization of the mKv1.2 K^+ channel subunit in different neurons of rat brain. J Neurosci 14:2408–2417.

Smart SL, Lopantsev V, Zhang CL, Robbins CA, Wang H, Chiu SY, Schwartzkroin PA, Messing A, Tempel BL (1998) Deletion of the Kv1.1 potassium channel causes epilepsy in mice. Neuron 20:809–819.

Southan AP, Robertson B (1998a) Patch-clamp recordings from cerebellar basket cell bodies and their presynaptic terminals reveal an asymmetric distribution of voltage-gated potassium channels. J Neurosci 18:948–955.

Southan AP, Robertson B (1998b) Modulation of inhibitory postsynaptic currents (IPSCs) in mouse cerebellar Purkinje and basket cells by snake and scorpion toxin K^+ channel blockers. Br J Pharmacol 125:1375–1381.

Tan YP, Llano I (1999) Modulation by K^+ channels of action potential evoked intracellular Ca^{2+} rises in rat cerebellar basket cells axons. J Physiol (Lond) 520:65–78.

Walmsley B, Alverez FJ, Fyffe REW (1998) Diversity of structure and function at mammalian central synapses. Trends Neurosci 21:81–88.

Wang H, Kunkel DD, Martin TM, Schwartzkroin PA, Tempel BL (1993) Heteromultimeric K^+ channels in terminal and juxtaparanodal regions of neurons. Nature 365:75–79.

Wang H, Kunkel DD, Schwartzkroin PA, Tempel BL (1994) Localization of Kv1.1 and Kv1.2, two K channel proteins, to synaptic terminals, somata, and dendrites in the mouse brain. J Neurosci 14:4588–4599.

Wang H-S, Pan Z, Shi W, Brown BS, Wymore RS, Cohen IS, Dixon JE, McKinnon D (1998) KCNQ2 and KCNQ3 potassium channel subunits: molecular correlates of the M-channel. Science 282:1890–1893.

Wang L-Y, Gan L, Forsythe ID, Kaczmarek LK (1998) Contribution of the Kv3.1 potassium channel to high-frequency firing in mouse auditory neurones. J Physiol (Lond) 509:183–194.

Wang WH, Strahlendorf JC, Strahlendorf HK (1991) A transient voltage-dependent outward potassium current in mammalian cerebellar Purkinje cells. Brain Res 567:153–158.

Weiser M, Vega-Saenz de Miera E, Kentros C, Moreno H, Franzen L, Hillman D, Baker H, Rudy B (1994) Differential expression of *Shaw*-related K^+ channels in the rat central nervous system. J Neurosci 14:949–972.

Yang W-P, Levesque PC, Little WA, Conder ML, Ramakrishnan P, Neubauer MG, Blanar MA (1998) Functional expression of two KvLQT1-related potassium channels responsible for an inherited idiopathic epilepsy. J Biol Chem 273:19419–19423.

Zhang C-L, Messing A, Chiu SY (1999) Specific alteration of spontaneous GABAergic inhibition in cerebellar Purkinje cells in mice lacking the potassium channels Kv1.1. J Neurosci 15:2852–2864.